Machine Learning Guided Development of Trialkylphosphine Ni$^{(I)}$ Dimers & Applications in Site-Selective Catalysis

Teresa M. Karl,[1] Samir Bouayad-Gervais,[1†] Julian A. Hueffel,[1†] Theresa Sperger,[1] Sebastian Wellig,[1] Sherif J. Kaldas,[1] Uladzislava Dabranskaya,[1] Jas S. Ward,[2] Kari Rissanen,[2] Graham J. Tizzard,[3] and Franziska Schoenebeck[1]*

[1]Institute of Organic Chemistry, RWTH Aachen University, Landoltweg 1, 52074 Aachen, Germany

[2]University of Jyvaskyla, Department of Chemistry, FIN40014, Jyväskylä, Finland

[3]UK National Crystallography Service, School of Chemistry, University of Southampton, SO17 1BJ Southhampton, United Kingdom

KEYWORDS: catalysis, speciation, nickel dimer, phosphine ligand, machine learning

ABSTRACT: Owing to the unknown correlation of a metal's ligand and its resulting preferred speciation in terms of oxidation state, geometry and nuclearity, a rational design of multinuclear catalysts remains challenging. With the goal to accelerate the identification of suitable ligands that form trialkylphosphine-derived dihalogen-bridged Ni$^{(I)}$ dimers, we herein employed an assumption-based machine learning approach. The workflow offers guidance in ligand-space for a desired speciation without (or only minimal) prior experimental data points. We experimentally verified the predictions and synthesized numerous novel Ni$^{(I)}$ dimers as well as explored their potential in catalysis. We demonstrate C-I selective arylations of polyhalogenated arenes bearing competing C-Br and C-Cl sites in under 5 min at room temperature using 0.2 mol% of the newly developed dimer, [Ni$^{(I)}$(μ-Br)PAd$_2$(*n*-Bu)]$_2$, which is so far unmet with alternative dinuclear or mononuclear Ni- or Pd catalysts.

INTRODUCTION

Bulky trialkylphosphine ligands, such as P(*t*-Bu)$_3$, have been transformative to the field of Pd-catalyzed cross coupling reactions, owing to their favoring of monophosphine Pd species in catalytic transformations, which in turn is imperative to reactivity and selectivity (Figure 1).[1] By contrast, the impact of these ligands in the closely related field of Ni-catalyzed coupling reactions is, comparably, much smaller,[2] which might be related to the differences in speciation of the two metals in terms of their accessible ligation and oxidation states. The putative key catalytic Pd$^{(0)}$L$_1$ species is frequently formed *in situ* from suitable Pd$^{(0)}$ precursors with readily displaceable auxiliary ligands, such as Pd$_2$dba$_3$. This strategy is not generally transferrable to the field of Ni-catalysis, however. For example, adding P(*t*-Bu)$_3$ to the widely employed precursor Ni(COD)$_2$ (in the absence or presence of a halogenated arene)[3] does not lead to COD-displacement; P(*t*-Bu)$_3$ and Ni(COD)$_2$ remain unchanged in solution (see Figure 1 & SI for details).[4,5] When suitable functionalities are present in the substrate, such as a carbonyl group, partial COD-displacement and formation of a carbonyl-bound Ni$^{(0)}$P(*t*-Bu)$_3$ species has been observed (in 17% yield) by Doyle.[6]

To enable *substrate-independent* access to Ni-species that carry bulky trialkylphosphine ligands therefore requires a different approach.[7] In the field of Pd-catalysis, dinuclear Pd$^{(I)}$ complexes of the form [Pd$^{(I)}$(*μ*-X)P(*t*-Bu)$_3$]$_2$ have been shown to be efficient pre-catalysts to Pd$^{(0)}$ species, if X = Br.[1,8,9] They constitute an attractive alternative to circumvent the above mentioned ligand exchange and also avoid reductive approaches

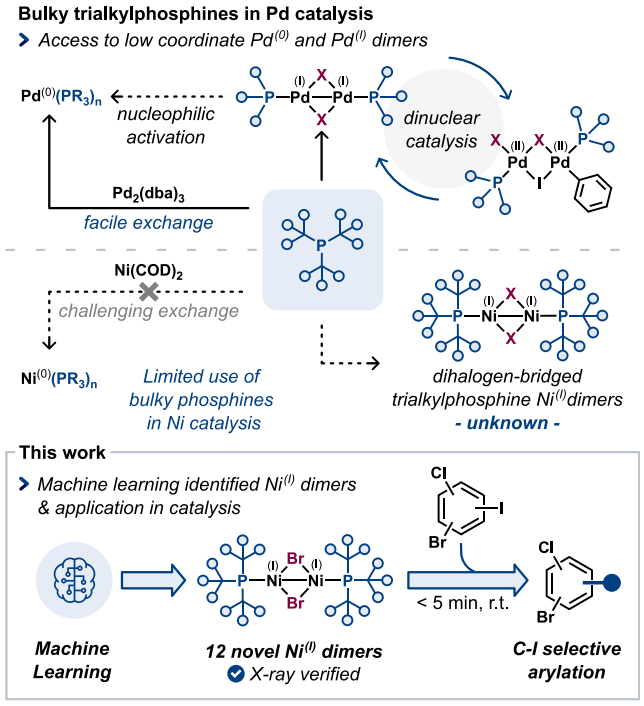

Figure 1. Differences of Ni- and Pd-catalysis in the chemistry with bulky trialkylphosphines, and this work.

from *e.g.* Pd$^{(II)}$ precursors, which can be accompanied with different speciation resulting in side-species that can influence the catalytic activity.[10] By contrast, for the Pd$^{(I)}$ dimer, the Pd$^{(0)}$

species is liberated directly through a nucleophile-induced disproportionation,[11] leading to a monophosphine $Pd^{(0)}$ species directly, which in turn gives rise to a dramatic rate acceleration in cross-coupling reactions as compared to alternative pre-catalysts.[5] Depending on the bridging halogen (X = Br is significantly more labile than X = I), $Pd^{(I)}$ dimers can also be direct catalysts, and knowledge has been gained over the past years on the factors that dictate the precise mechanistic role.[8b,10a,11,12]

Although oxidation state one is much more common for Ni than Pd and numerous $Ni^{(I)}$ complexes (monomeric as well as dimeric)[13] have been isolated and characterized,[7b,14] the analogous dihalogen-bridged $Ni^{(I)}$ dimers carrying such bulky trialkyl-phosphine ligands are so far unexplored.[15] NHC-based dihalogen-bridged $Ni^{(I)}$ dimers have been reported[16] and have been shown to display promising reactivities.[17]

In light of the significant potential to be direct catalysts[17a,b] or efficient precursors, and hence the prospect of potentially enabling straightforward and substrate-independent access to trialkylphosphine bound Ni-catalytic species, we set out to explore dihalogen-bridged trialkylphosphine $Ni^{(I)}$ dimers. To accelerate the identification of suitable ligands that would favor the desired oxidation state, geometry and nuclearity, we employed machine learning[6,18-20] and subsequently experimentally investigated the algorithm-suggested candidates. This approach led to several dihalogen-bridged trialkylphosphine derived $Ni^{(I)}$ dimers. We also explored the potential of these new dimers to address pertinent challenges in catalysis and demonstrated the iodo-selective arylation of arenes that also carry C-Br and C-Cl competing sites, which is so far unmet with mono- and dinuclear Ni and Pd catalysts.[21]

RESULTS & DISCUSSION

Unsupervised Machine Learning Workflow

As $Ni^{(I)}$ complexes can occur in various geometries and nuclearities (monomeric or dimeric),[13] and as there is currently no rationale available to derive the impact of a given ligand on the speciation, we initially set out to explore which bulky trialkylphosphine ligands might be suitable candidates to ultimately form the desired $Ni^{(I)}$ dimers. We recently reported the potential of machine learning to address such speciation challenges in the context of $Pd^{(I)}$ dimer formation.[22] Using only a handful of experimental data points paired with *in silico* data acquisition and ligand databases, we were able to identify ligands that give rise to $Pd^{(I)}$ dimers of analogous geometry and properties.

We had started our investigation from an *in silico* generated database of 348 monodentate phosphine ligands, developed by Fey, Harvey, Orpen and colleagues (so-called LKB-P).[18g,23] The database contains information on the ligand properties and their interactions in different model complexes, aiming to reflect a ligand's properties as generally as possible with a multidimensional parameterization approach. About 1/3 of the ligands in the database are non-commercial or have never been made, underscoring the potential of this approach to also explore novel phosphine space for the problem at hand. We had initially clustered the LKB-P with the *k*-means algorithm[24] on the basis of their general properties (*i.e.* the descriptors in the database). This allowed to identify groups of ligands that feature the same general characteristics. We then proceeded with those clusters that contained the four known Pd-dimer-forming trialkylphosphines and disregarded the other clusters. (At this point there is in principle the possibility to test representative ligands of the other clusters to potentially identify more 'positive clusters' and hence more ligands). Following this initial 'filtering', the remaining ligands that were grouped with the positive references (= 66) were subsequently parametrized with DFT-based descriptors related to the specific problem of Pd speciation and re-subjected to the clustering algorithm. Overall, this sequential clustering strategy led to the prediction of several new ligands, including never made ones, which we subsequently verified experimentally. We envisioned that the analogous machine-learning approach could be similarly enabling to identify trialkylphosphine based dihalogen-bridged $Ni^{(I)}$ dimers.

A key challenge in transferring our approach to Ni-speciation arises from the absence of any known dihalogen-bridged trialkylphosphine-based $Ni^{(I)}$ dimer, which in turn could be used as a reference for our unsupervised-machine learning workflow. As a first approximation, we therefore decided to consider the same 66 ligand subspace that originated from the LKB-P clustering and contained the ligands that are similar to bulky trialkyl phosphines, such as P(*t*-Bu)$_3$ and PAd$_2$(*n*-Bu). To further subcategorize the 66 ligands, we then provided *guesses* to the algorithm by assuming/assigning that a certain ligand will lead to a $Ni^{(I)}$ dimer of the desired geometry, while another ligand will not (Figure 2C). We labelled P(*t*-Bu)$_3$ as a pseudo-positive reference in this context. As a pseudo-negative reference, we chose tri(neopentyl)phosphine since our prior work showed that it does not form a $Pd^{(I)}$ dimer.[22] Given the smaller size of Ni as compared to Pd, and the fact that Br-bridges made $Pd^{(I)}$ dimers excellent pre-catalysts, we decided to focus our search on Br-bridged $Ni^{(I)}$ dimers.

By analogy to our previous report,[22] we introduced problem-specific descriptors for the 66 ligands to guide the selection process to the specific task of identifying ligands similar to P(*t*-Bu)$_3$ that would generate a dihalogen-bridged $Ni^{(I)}$ dimer species. The descriptors were generated *in silico* through quantum mechanical (DFT) calculations (see SI for details). To this end, we calculated various features of the free ligands, mono- and bisligated $Ni^{(0)}$, $Ni^{(I)}$ and $Ni^{(II)}$ complexes as well as the desired dibromo-bridged $Ni^{(I)}$ dimer.

As a result, we obtained 184 descriptors (as compared to the 42 we previously derived in the case of palladium)[22] that capture the electronic and steric effects of the different phosphines related to nickel speciation. The number (and in part also type) of calculated descriptors differ from our previous study with $Pd^{(I)}$, as we have meanwhile generated an *in-house* automated workflow, which allows to readily generate a multitude of descriptors rapidly. Moreover, while we have previously involved structural descriptors such as bond distances, angles and Sterimol parameters to describe sterics in Pd speciation, this time we additionally included percent buried volume (%V_{bur}), accessible molecular surface (AMS), bond vibration frequencies, and several more (see SI for details).

Since the construction of machine learning models generally requires the number of features/descriptors to be less than the number of samples in a dataset,[25] we subsequently set out to lower the feature dimensionality (Figure 2D). We applied Pearson correlation coefficient analysis in the selection process and removed those features exceeding 90% correlation, which resulted in a total number of 126 descriptors. Subsequently, we analyzed how well each descriptor separated the pseudo-positive and pseudo-negative references.

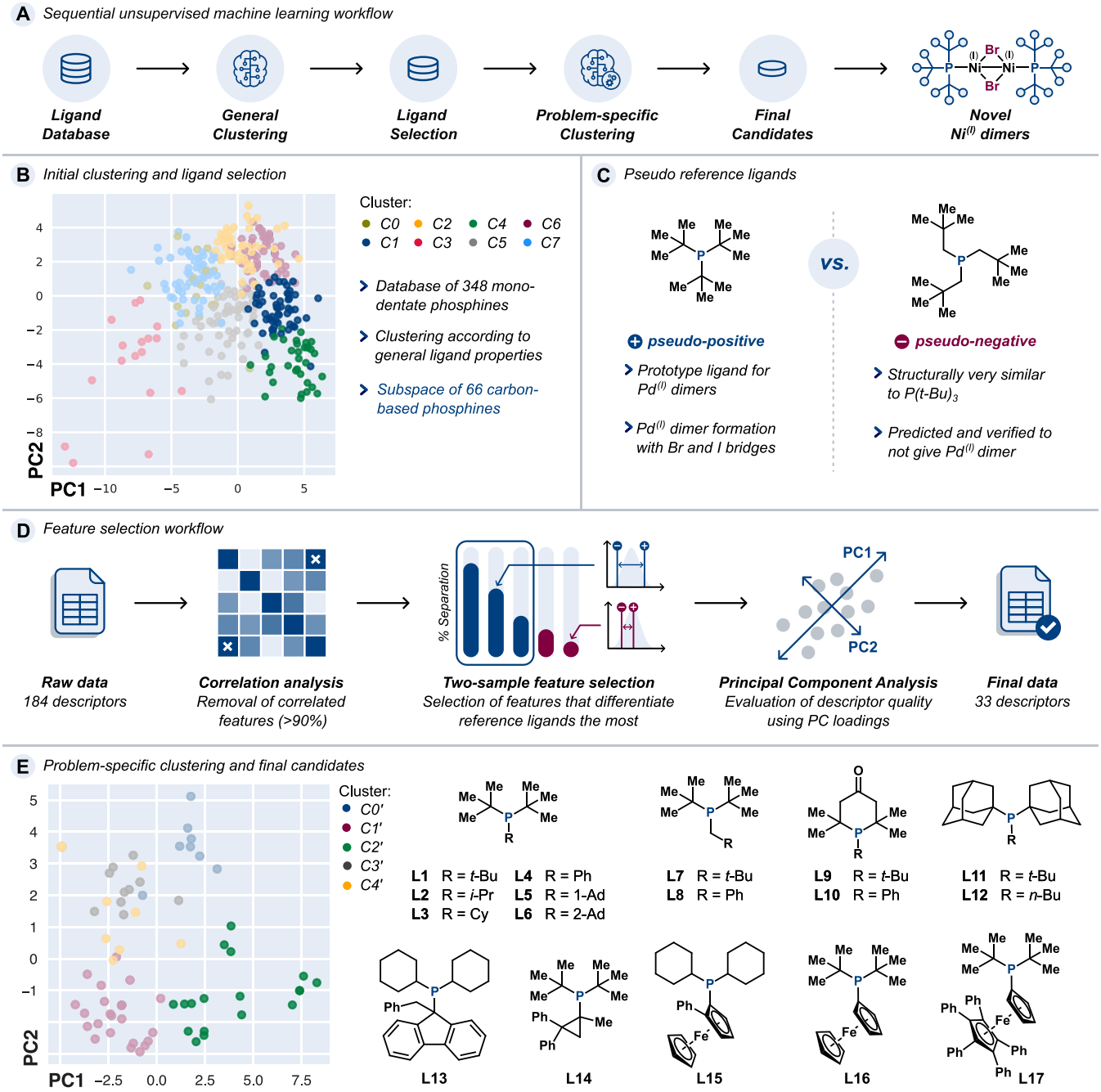

Figure 2. A) Overview of the sequential clustering workflow with problem-specific refinement. B) Results of the initial clustering[18]. C) Pseudo-reference ligands. D) Illustration of the feature selection workflow using pseudo-references (see SI for details). E) Results of the problem-specific clustering and final candidates for $Ni^{(I)}$ dimer formation.

We decided to focus on the 33 descriptors that provide the widest differentiation between these reference ligands, so that the number of features was overall half the number of ligands in our dataset. Subsequently, principal component analysis (PCA) was performed to obtain an appropriate representation of the problem-specific feature space and to verify the contribution of each of the chosen descriptors to the variance in the dataset (see SI).

Following the generation of the problem-specific data, we proceeded with *k*-means clustering. On the basis of the elbow method as well as average and per-sample silhouette scores and Davies-Bouldin-score, the cluster number $k = 5$ was chosen. The default number of centroid seeds was set at 5000 to ensure that the resulting clusters represent the best possible fit to our data. To account for potential statistical fluctuation in our results, the clustering was performed 1000 times using different random states, tracking how many times a ligand was stored in the same cluster as the pseudo-positive reference, *i.e.*, was part of the final candidates (see SI for details). With this approach, the algorithm grouped 15 phosphine ligands together with P(*t*-

$Bu)_3$ (cluster C2', Figure 2E) in 100% of cases and one ligand (**L17**) in >80% of the 1000 clusterings. These 16 candidates (in addition to P(*t*-Bu_3)) include various bulky trialkyl phosphines (*e.g.* **L1 - L8**), but also ferrocenyl-containing phosphines (**L15 - L17**) as well as constrained phosphinanone derivatives (**L9/10**). Interestingly, for several of these ligands there appear to be no reports of uses in the field of Ni-catalysis (*e.g.* **L3**, **L8, L9**, **L13**, **L16**).[6,26] In fact, for **L13** there are, to the best of our knowledge, only two reports of a use in catalysis in general (for any metal, in this case with Pd),[27] and **L9** had never even been made before our recent exploration with $Pd^{(I)}$ dimers.[22] This reflects a key-benefit of the machine learning-based workflow (*i.e.* database-mining) as being able to assess ligand space that might be completely unknown or unexplored.

The pseudo-negative reference was stored among seven other ligands in a separate cluster (cluster C4'). Another cluster contained a variety of smaller alkyl- as well as aryl-phosphines (cluster C1') whereas Buchwald-type biaryl phosphines were found in two clusters (Cluster C0' and C3') (see SI for all the clusters and their ligands).

$Ni^{(I)}$ Dimer Synthesis

We next set out to attempt the synthesis of $Ni^{(I)}$ dimers with the predicted ligands. To this end, we adapted the procedure known to form NHC-based dihalogen-bridged $Ni^{(I)}$ dimers,[16] which relies on a comproportionation approach of $Ni^{(0)}$ and $Ni^{(II)}$ species. While trialkylphosphine ligands do not efficiently displace COD from $Ni(COD)_2$ (as discussed above), we reasoned that $Ni(COD)_2$ and $NiBr_2$ might undergo comproportionation and the resulting species may then be prone to COD displacement by the phosphine, as work by Krossing has shown that electron deficient $Ni(COD)_2^+$ would undergo COD-displacement with trialkylphosphines.[4]

The addition of $NiBr_2$(dme) to a solution of $Ni(COD)_2$ and the trialkylphosphine ligand PAd_2(*n*-Bu) (**L12**) in THF and additional stirring for 1 min at r.t. led to a color change from yellow to green. Our subsequent crystal growth through vapor diffusion (hexane/THF) at -30 °C pleasingly led to suitable crystals for X-ray crystallographic analysis within two days, which confirmed the formation of the dibromo-bridged $Ni^{(I)}$ dimer **D12** (see Figure 3). Further analysis by ^{31}P NMR spectroscopy showed a signal at 64.1 ppm upon dissolving the dimer in benzene. While only a single signal in ^{31}P NMR was observed, there is remaining uncertainty as to whether the dimeric form observed in the solid state is retained in solution. We therefore turned to computational studies to calculate the expected ^{31}P NMR chemical shift of the dimer as well as alternative species.

The accurate reproduction of absolute chemical shifts using DFT is challenging. However, the relative shift change, *i.e.* by how many ppm a signal would shift for a ligand when bound to a metal ($= \delta_{NiL}$) compared to its free form ($= \delta_L$), can be predicted with much greater precision (see SI for details).[28]

Our calculations predicted a ^{31}P NMR shift of $\delta_{NiL} - \delta_L = 43$ ppm for $Ni^{(I)}$ dimer **D12**, which was very close to the measurement in benzene ($\delta_{NiL} - \delta_L = 39$ ppm). Notably, THF has a pronounced impact on the ^{31}P NMR shift as dissolving the same dimer in THF leads to a 20 ppm more downfield signal at 84.1 ppm.

Applying the same comproportionation-based synthesis in THF and also in benzene[29] for the trialkylphosphine ligands P(*t*-$Bu)_2$(*i*-Pr) (**L2**), P(*t*-$Bu)_2$Cy (**L3**) and P(*t*-$Bu)_2$Bn (**L8**) as well as the more unusual phosphinanone **L9**, we saw the analogous color changes to green taking place upon $NiBr_2$(dme) addition to the $Ni(COD)_2$/phosphine solution, while for QPhos (**L17**) the mixture stayed deep red. The ^{31}P NMR analyses of the reaction mixtures in THF and in benzene showed a defined new signal in each case, indicating that a new species had formed for each of these ligands also. The measured ^{31}P NMR shifts of the newly formed species in benzene resembled those calculated for the corresponding $Ni^{(I)}$ dimers very well, deviating only by 1- 5 ppm (see Figure 3).[30] Our attempts to grow crystals in these cases were successful and we unambiguously confirmed the formation of dibromo-bridged $Ni^{(I)}$ dimers **D2**, **D3**, **D8, D9** and **D17** by X-ray crystallography (for details see SI).[31]

The analogous synthesis attempts involving P(*t*-$Bu)_2$Ph (**L4**), P(*t*-$Bu)_2$(2-Ad) (**L6**), PCy_2BnFlu (**L13**) and the dialkylaryl analogue P(*t*-$Bu)_2[FeCp_2]$ (**L16**) also led to a single observable species in each case, as judged by ^{31}P-NMR measurement. Although the calculated ^{31}P-NMR shifts of the corresponding dimers deviated from the measured signals in benzene by 10-16 ppm,[32] **D4**, **D6, D13** and **D16** could also be unambiguously confirmed by X-ray crystallography (Figure 3).[31 33]

Interestingly, when we employed P(*t*-$Bu)_2$Ad (**L5**) in the synthesis, one dominant species[34] was also observed by ^{31}P NMR. However, it was surprisingly downfield and observed at 142.0 ppm in benzene (and 167.9 ppm in THF). Our DFT calculations suggested 105.7 ppm for the corresponding $Ni^{(I)}$ dimer **D5** in benzene, which as opposed to the above discussed cases is a substantial deviation by 36 ppm. Despite this discrepancy, X-ray crystallographic analysis revealed that $[Ni^{(I)}(\mu\text{-Br})P(t\text{-}Bu)_2Ad]_2$ (**D5**) had formed (Figure 3). The analogous discrepancy was observed also for P(*t*-$Bu)_2$Np **L7**, for which a ^{31}P-NMR signal at 121.5 ppm in benzene (and 143.0 ppm in THF) was observed in our attempted dimer synthesis (along with remaining free ligand), deviating by 44 ppm from our computational predictions for **D7**. Yet, the corresponding $Ni^{(I)}$ dimer **D7** could be confirmed in the solid-state by X-ray crystallographic analysis.[31] We speculate that the downfield ^{31}P NMR shifts of the dissolved dimers might potentially indicate a disparity between the solid state and solution state speciation in these cases.

Our analogous attempts to synthesize a $Ni^{(I)}$ dimer with P(*t*-$Bu)_3$ (**D1**) similarly resulted in an instantaneous color change of the reaction mixture to green. Our analysis of the reaction mixture gave a dominant ^{31}P NMR signal at 128.7 ppm in benzene (and 147.6 ppm in THF) alongside free ligand. Also here, DFT predicted a 20 ppm more upfield shift (108.5 ppm).

In stark contrast, our attempted $Ni^{(I)}$ dimer synthesis with PAd_2(*t*-Bu) (**L11**) led to the immediate formation of an insoluble blue-green solid, which could not be further analyzed. It therefore remains inconclusive whether the obtained solid is the desired $Ni^{(I)}$ dimer. (Our problem-specific data did not include descriptors that characterize solubility.) On the other hand, for the $Ni^{(I)}$ dimer synthesis with phosphinanone **L10**, the ^{31}P NMR analysis gave no signal, which might indicate that a paramagnetic species resulted in this case, *e.g.* a monomeric $Ni^{(I)}$, contrasting the observations with the structurally very similar **L9**, for which we obtained the dimer **D9**. For cBRIDP ligand **L14**, there was no change observed in the ^{31}P NMR spectrum upon attempted $Ni^{(I)}$ dimer synthesis. Only free ligand was seen.

The bulkiness of this particular ligand makes its coordination to a metal challenging; indeed our previous attempts to synthesize a $Pd^{(0)}$ complex with this ligand bound to it had also failed.[22] The ligand might also be too bulky to displace COD in our present attempts. Consequently, the lack of indication of $Ni^{(I)}$ dimer

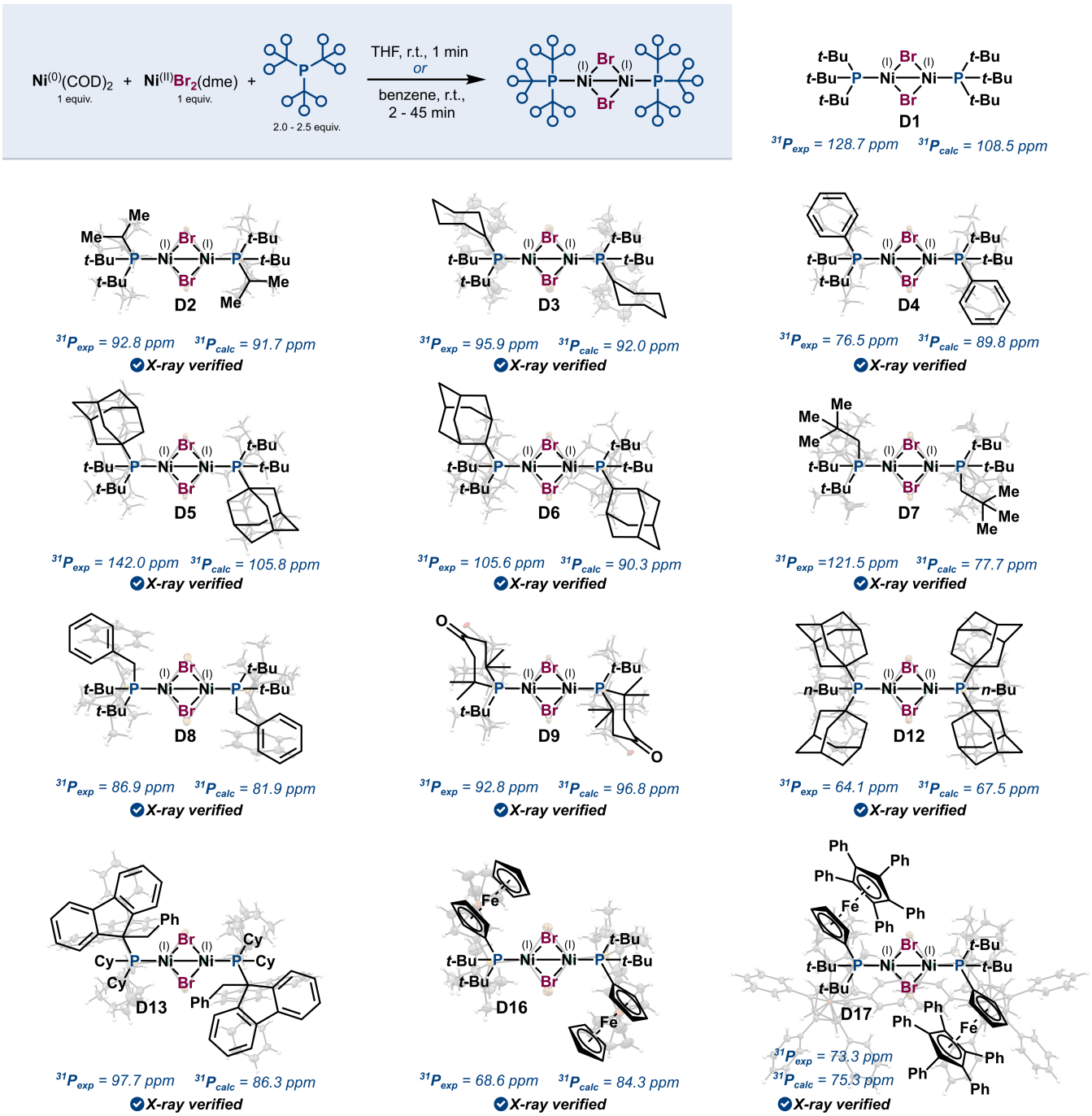

Figure 3. Synthesis of $Ni^{(I)}$ dimers via comproportionation: In THF, $NiBr_2$(dme) is added to a solution of $Ni(COD)_2$ and phosphine within 1 min. After 1 min of stirring, aliquots for ^{31}P NMR analysis were taken. The corresponding NMR shifts are reported in the SI. In benzene, $NiBr_2$(dme) and phosphine were mixed and stirred for 45 min – 4 h. Then, $Ni(COD)_2$ in benzene was added dropwise and stirred for 2 – 45 min prior to ^{31}P NMR analysis. Experimental and DFT-calculated ^{31}P NMR shifts for the detected nickel-ligand complexes ($^{31}P_{exp}$ and $^{31}P_{calc}$, respectively) are given in benzene. X-ray structures of **D2-D9, D12, D13, D16** and **D17** are shown in a shaded way behind the structures (for details see SI).[31]

formation in this case may not necessarily reflect an inability of the ligand to stabilize $Ni^{(I)}$ but instead the challenges associated with ligand exchanges as a result of the chosen precursors and synthetic route. For our pseudo-negative reference tri(neopentyl)phosphine (**L19**), the same synthesis effort did not result in a new ^{31}P NMR signal, but gave black nickel flakes alongside free ligand.

Overall, our synthesis attempts with the algorithm-predicted ligands led to numerous dibromo-bridged $Ni^{(I)}$ dimers. The algorithm identified ligands that have so far only found limited, if any, prior use in Ni-catalysis, which underscores the value of this workflow to identify ligands for which no experimental data currently exists. This approach therefore offers a means to

accelerate the identification of ligand candidates through filtering the vast possible ligand space, and the various clusters can further be evaluated with representative candidates to increase the number of predictions. Our chosen approach focused on identifying ligands that are 'similar' to P(*t*-Bu)$_3$ and a P(*t*-Bu)$_3$-derived bromine-bridged Ni$^{(I)}$ dimer with the overarching goal and assumption that the multiparameter-based similarity of ligand will ultimately also lead to similar structure/speciation and reactivity. (Our approach was not directed at identifying all possible ligands for Ni$^{(I)}$ dimer formation.)

As X-ray crystallography is ultimately required to unambiguously prove the identity (and structure) of the Ni$^{(I)}$ dimers, alternative approaches *via e.g.* high-throughput screening would not lead to the identification of new dimers any faster than trial-and-error experimentation. Moreover, our approach allows to assess ligand space that is currently unknown (*i.e.* never synthesized or non-commercial).

Ni$^{(I)}$ Dimer Application

With these novel complexes in hand, we subsequently set out to investigate their potential in catalysis. The selective functionalization of polyhalogenated arenes is of significant interest as it enables a rapid and modular approach to diversely substituted arenes.[35] In this context, our group showed that the dinuclear complex [Pd$^{(I)}$(μ-I)P(*t*-Bu)$_3$]$_2$ enables a substrate-independent and *a priori* predictable functionalization of C-Br bonds in the presence of C-OTf (or C-OSO$_2$F) and C-Cl bonds in poly(pseudo)halogenated arenes at r.t. in less than 5 min reaction time.[36] However, the same Pd$^{(I)}$ dimer was unable to discriminate C-I from C-Br. The exclusive functionalization of C-I bonds in the presence of C-Br and C-Cl bonds could only be achieved using a Pd trimer.[21]

In the context of Ni-catalyzed cross couplings chemoselective C-I bond alkylation of polyhalogenated arenes was recently achieved with Ni/photoredox dual catalysis following a radical mechanism employing a Ru-based photocatalyst and an alkylsilicate as transmetalation agent within 16 h at room temperature.[37] Arylation was not amenable to the latter approach however. Other isolated examples of C-I selective alkylations have also been reported as part of method developments, involving reductive cross-couplings.[38] Similarly, our group showed a few examples of C-I selective C-SeCF$_3$ couplings (in the presence of competing C-Br or C-Cl sites) involving a NHC-based Ni$^{(I)}$ dimer and likely dinuclear catalysis.[17a]

In light of the promising prior findings for Ni$^{(I)}$ as well as the ever-growing interest in greater sustainability and hence catalysis with less-precious metals, we wondered whether selective arylations could potentially be achieved using our newly developed trialkylphosphine derived Ni$^{(I)}$ dimers. To this end, we mixed the di(adamantanyl)(butyl)-phosphine-derived dimer **D12** at r.t. with aryl Grignard and the electrophile in THF. We observed selective C-I couplings in the presence of C-Br (and C-Cl) in under 5 min reaction time. Our further studies revealed that 0.2 mol% of the catalyst **D12** was sufficient to selectively arylate the C-I bond of numerous substrates (see **1** - **13**, Figure 4).[39]

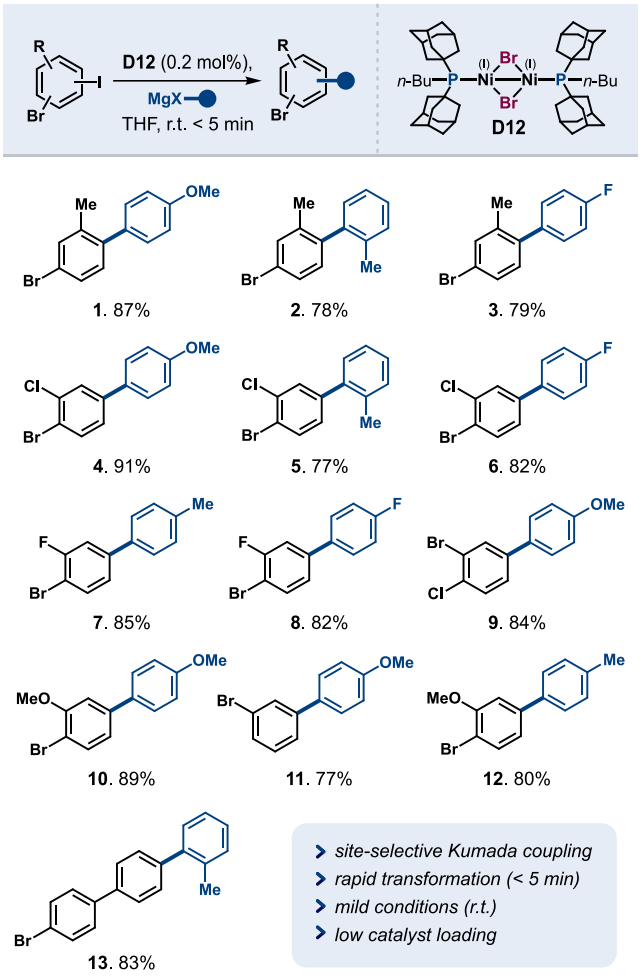

Figure 4. Scope of the Kumada cross coupling with Ni$^{(I)}$ dimer **D12** as the catalyst. Reaction conditions: aryl halide (1.0 equiv.), Grignard reagent (1.0 equiv.), **D12** (0.2 mol%) in THF (0.4 M). Yields of isolated products are given.

Electron-poor and electron-rich substrates rapidly reacted with both electron-rich and electron-poor Grignard reagents. Substituents in *ortho*-position to the C-I bond (**1**, **2**, **3**) were also tolerated. Polyhalogenated substrates (**4** - **9**) carrying additional -Cl or -F substituents were also selectively coupled at C-I to deliver the cross-coupling products in good yields. Additional functionalities such as halogen-substituents (**3**, **6**, **8**) or methoxy-groups (**1**, **4**, **9** - **11**) could also readily be introduced via the Grignard reagents.

Given the high reactivity (less than 5 min at r.t.) and the high C-I selectivity, we wondered what species might potentially be reactive. The cross-coupling reactions proceed equally well in benzene. Upon mixing Ni$^{(I)}$ dimer **D12** (1 equiv.) with substrate 1-bromo-4-iodo-2-methoxybenzene (2 equiv.) in benzene or THF, a second signal is observed upon immediate analysis by ^{31}P NMR spectroscopy.[40] However, the majority of the dimer stays untouched and 94% of the iodo arene remained unreacted in benzene (88% in THF). The remainder of the material resulted in homocoupled starting material, which was not seen under the catalytic coupling conditions however (or if at all, only in traces, see SI). On the other hand, addition of 2 equiv. of Grignard reagent (*i.e. p*-tolylmagnesium bromide) to 1 equiv. of **D12** leads to immediate consumption of **D12** and formation of a new phosphine-containing species.[41]

This parallels our prior observations with $Pd^{(I)}$ dimers, which similarly form a new species instantaneously upon exposure to the organometallic reagent. A bimetallic complex of oxidation state one could result that incorporates carbon bridges. Indeed, such a species has been successfully characterized for NHC based $Ni^{(I)}$ dimers.[17b] However, it cannot be ruled out that alternative species might be liberated in the process, such as $Ni^{(0)}PR_3$. Our experiments employing $Ni(COD)_2$[42] or $Ni(COD)_2$/ PAd_2(*n*-Bu) or [(TMEDA)Ni(*o*-tol)Cl]/PAd_2(*n*-Bu) (**14**) in couplings of 1-bromo-2-chloro-4-iodobenzene with 4-methoxyphenyl-magnesium bromide did not lead to formation of coupling product (**4**) within the same reaction time. Instead, only unreacted starting material was observed. Similarly, employment of the same catalyst/ligand combinations to the coupling of 1-bromo-4-iodo-2-methoxybenzene with *p*-tolylmagnesium bromide (to form **12**) resulted in an analogous outcome for $Ni(COD)_2$ and **14** and only 5% of product formation alongside unreacted starting material when using $Ni(COD)_2$/PAd_2(*n*-Bu). Extension of reaction time barely led to more formation of product; significant de-iodination of starting material (presumably due to competing metal halogen exchange) was instead dominant.[43]

Collectively, these results suggest that the reactive species derived from the $Ni^{(I)}$ dihalogen-bridged dimer **D12** is either unique or less readily accessible when starting from $Ni(COD)_2$ or $Ni^{(II)}$ complex **14**. The data does not allow to unambiguously differentiate between $Ni^{(0)}$ or $Ni^{(I)}$ dimer catalysis (or alternatives), however. Nevertheless, to the best of our knowledge, the first C-I selective arylation (in competition with C-Br) was accomplished under Ni-catalysis.

CONCLUSIONS

In summary, this work focused on the development of trialkylphosphine-derived dibromo-bridged $Ni^{(I)}$ dimers for potential applications in catalysis as either direct catalysts or as pre-catalysts to trialkylphosphine-bound $Ni^{(0)}$ species. The latter $Ni^{(0)}$ complexes are otherwise not readily accessible from commonly used precursors, such as $Ni(COD)_2$, owing to a lack (or low efficiency) of COD-displacement by bulky trialkylphosphines, such as P(*t*-Bu)$_3$. As the required ligand properties and overall factors that dictate Ni-speciation in terms of favored oxidation state, geometry and nuclearity are currently unknown, we employed machine learning to identify suitable ligands. To this end, we performed sequential *k*-means clustering of a database of phosphine ligands that was complemented with *in-silico* generated (*i.e.* DFT calculated) problem-specific data. Owing to the absence of any known trialkylphosphine-derived dihalogen-bridged $Ni^{(I)}$ dimers, we provided *guesses* as positive and negative ligand references to guide the clustering and identify ligands that are similar to our positive reference for the speciation problem at hand. While the workflow, as conducted, is not exhaustive in identifying all possible ligands for $Ni^{(I)}$ dimers (which it has the potential to be however, if complemented with experimental tests), it led to 17 suggested ligands, many of which have not found any prior use in Ni-catalysis. We experimentally tested these candidates, and overall were able to unambiguously confirm by X-ray crystallography the identity of 12 dibromo-bridged $Ni^{(I)}$ dimers. For several of these dimers our calculated ^{31}P-NMR data also agreed with the measurements of the dissolved dimers in benzene. We also explored their potential in catalysis and observed the iodo-selective arylation of polyhalogenated arenes that contain competing C-I, C-Br and C-Cl sites in less than 5 min reaction time at room temperature with 0.2 mol% loading of $[Ni^{(I)}(\mu\text{-Br})PAd_2(n\text{-Bu})]_2$. Such selectivity paired with high speed has not previously been achieved for arylations of C-I bonds in such competition scenarios with alternative mono- or dinuclear Pd or Ni catalysts. Overall, this work further manifests the power of applying machine learning to accelerate the identification of new catalysts from currently unknown or unexplored ligand-space.

ASSOCIATED CONTENT

Supporting Information. The Supporting Information is available free of charge at http://pubs.acs.org
Computational details, data generation and analysis, experimental details, characterization of compounds, crystallographic data.

Accession Codes. CCDC 2265372 (**D2**), 2252179 (**D3**), 2265373 (**D4**), 2252180 (**D5**), 2265374 (**D6**), 2265375 (**D7**), 2252146 (**D8**), 2265472 (**D9**), 2252211 (**D12**), 2252181 (**D13**) and 2252147 (**D16**), 2265376 (**D17**) contain the supplementary crystallographic data for this paper. These data can be obtained free of charge via www.ccdc.cam.ac.uk/data_request/cif, or by emailing data_request@ccdc.cam.ac.uk, or by contacting The Cambridge Crystallographic Data Centre, 12 Union Road, Cambridge CB2 1EZ, UK; fax: +44 1223 336033.

AUTHOR INFORMATION

Corresponding Author

*Franziska Schoenebeck – Institute of Organic Chemistry, RWTH Aachen University, 52074 Aachen, Germany; orcid.org/0000-0003-0047-0929; Email: franziska.schoenebeck@rwth-aachen.de

Authors

Teresa M. Karl – Institute of Organic Chemistry, RWTH Aachen University, 52074 Aachen, Germany

Samir Bouayad-Gervais – Institute of Organic Chemistry, RWTH Aachen University, 52074 Aachen, Germany

Julian A. Hueffel – Institute of Organic Chemistry, RWTH Aachen University, 52074 Aachen, Germany; orcid.org/0000-0001-6218-8502

Theresa Sperger – Institute of Organic Chemistry, RWTH Aachen University, 52074 Aachen, Germany; orcid.org/0000-0002-3870-9870

Sebastian Wellig – Institute of Organic Chemistry, RWTH Aachen University, 52074 Aachen, Germany

Sherif J. Kaldas – Institute of Organic Chemistry, RWTH Aachen University, 52074 Aachen, Germany; orcid.org/0000-0003-2497-1963

Uladzislava Dabranskaya – Institute of Organic Chemistry, RWTH Aachen University, 52074 Aachen, Germany

Jas S. Ward – University of Jyvaskyla, Department of Chemistry, FIN40014, Jyväskylä, Finland; orcid.org/0000-0001-9089-9643

Kari Rissanen – University of Jyvaskyla, Department of Chemistry, FIN40014, Jyväskylä, Finland; orcid.org/0000-0002-7282-8419

Graham J. Tizzard – UK National Crystallography Service, School of Chemistry, University of Southampton, SO17 1BJ Southhampton, United Kingdom; orcid.org/0000-0002-1577-5779

Author Contributions

†S. B.-G. and J. A. H. contributed equally.

Notes

The authors declare no competing financial interest.

ACKNOWLEDGMENT

We thank RWTH Aachen University, the European Research Council (ERC-637993), the Volkswagen Foundation (Momentum Program), the DFG (German Research Foundation) Cluster of Excellence 2186 ("The Fuel Science Center" – ID: 390919832) and the Fonds der Chemischen Industrie (Kekulé scholarship to T. M. Karl) for funding. Calculations were performed with computing resources granted by JARA-HPC from RWTH Aachen University under project "jara0091". We thank Prof. Abigail Doyle for stimulating discussions.

REFERENCES

(1) For reviews, see: (a) Christmann, U.; Vilar, R. Monoligated Palladium Species as Catalysts in Cross-Coupling Reactions. *Angew. Chem. Int. Ed.* **2005**, *44*, 366-374; (b) Hartwig, J. F. *Organotransition Metal Chemistry: from Bonding to Catalysis*; University Science Books: Sausalito, California, USA, 2010, p 877-966; (c) Shaughnessy, K. H. Development of Palladium Precatalysts that Efficiently Generate LPd(0) Active Species. *Isr. J. Chem.* **2020**, *60*, 180-194; (d) Firsan, S. J.; Sivakumar, V.; Colacot, T. J. Emerging Trends in Cross-Coupling: Twelve-Electron-Based $L_1Pd(0)$ Catalysts, Their Mechanism of Action, and Selected Applications. *Chem. Rev.* **2022**, *122*, 16983-17027.

(2) (a) Rosen, B. M.; Quasdorf, K. W.; Wilson, D. A.; Zhang, N.; Resmerita, A.-M.; Garg, N. K.; Percec, V. Nickel-Catalyzed Cross-Couplings Involving Carbon–Oxygen Bonds. *Chem. Rev.* **2011**, *111*, 1346-1416; (b) Jana, R.; Pathak, T. P.; Sigman, M. S. Advances in Transition Metal (Pd,Ni,Fe)-Catalyzed Cross-Coupling Reactions Using Alkyl-organometallics as Reaction Partners. *Chem. Rev.* **2011**, *111*, 1417-1492; (c) Montgomery, J. *Organonickel Chemistry*; Wiley: Hoboken, 2013, p 319-428; (d) S. Z. Tasker; E. A. Standley; T. F. Jamison. Recent advances in homogeneous nickel catalysis. *Nature* **2014**, *509*, 299-309.

(3) We used 1-chloro-4-fluorobenzene in our investigation, see SI.

(4) By contrast, $Ni(COD)_2^+$ does undergo efficient COD displacement to form $Ni(PR_3)_2^+$, see: (a) Schwab, M. M.; Himmel, D.; Kacprzak, S.; Kratzert, D.; Radtke, V.; Weis, P.; Ray, K.; Scheidt, E.-W.; Scherer, W.; de Bruin, B.; Weber, S.; Krossing, I.. $[Ni(cod)_2][Al(OR^F)_4]$, a Source for Naked Nickel(I) Chemistry. *Angew. Chem. Int. Ed.* **2015**, *54*, 14706-14709; (b) Schwab, M. M. ; Himmel, D.; Kacprzak, S.; Radtke, V.; Kratzert, D.; Weis, P.; Wernet, M.; Peter, A.; Yassine, Z.; Schmitz, D.; Scheidt, E.-W.; Scherer, W.; Weber, S.; Feuerstein, W.; Breher, F.; Higelin, A.; Krossing, I. Synthesis, Characterisation and Reactions of Truly Cationic Ni^I–Phosphine Complexes. *Chem. Eur. J.* **2018**, *24*, 918-927.

(5) More stable alternatives to $Ni(COD)_2$ have been developed, the challenge of auxiliary displacement remains also for these species. For example, see: (a) Nattmann, L.; Saeb, R.; Nöthling, N.; Cornella, J. An air-stable binary Ni(0)–olefin catalyst. *Nature Catal.* **2020**, *3*, 6-13; (b) Tran, V. T.; Kim, N.; Rubel, C. Z.; Wu, X.; Kang, T.; Jankins, T.C.; Li, Z.-Q.; Joannou, M. V.; Ayers, S.; Gembicky, M.; Bailey, J.; Sturgell, E. J.; Sanchez, B. B.; Chen, J. S.; Lin, S.; Eastgate, M. D.; Wisniewski, S. R.; Engle, K. . Structurally Diverse Bench-Stable Nickel(0) Pre-Catalysts: A Practical Toolkit for In Situ Ligation Protocols. *Angew. Chem. Int. Ed.* **2023**, *62*, e202211794.

(6) Newman-Stonebraker S., H.; Smith S., R.; Borowski J., E.; Peters, E.; Gensch, T.; Johnson H., C.; Sigman M., S.; Doyle A., G. Univariate classification of phosphine ligation state and reactivity in cross-coupling catalysis. *Science* **2021**, *374*, 301-308.

(7) While arene coordinated labile Ni(0)L species have been developed, which circumvent the COD-displacement challenge, such complexes do not yet exit for bulky trialkylphosphines and prior literature commented on such synthesis attempts to have been challenging or complexes only to be stable below -30 °C, see: (a) Nickel, T.; Goddard, R.; Krüger, C.; Pörschke, K.-R. Cyclotrimerization of Ethyne on the Complex Fragment $[(\eta^1\text{-}t\text{Bu}_2\text{PCH}_2\text{P}t\text{Bu}_2)\text{Ni}^0]$ with Formation of an η^6-Benzene-Nickel(0) Complex. *Angew. Chem. Int. Ed.* **1994**, *33*, 879-882; (b) Beck, R.; Shoshani, M.; Krasinkiewicz, J.; Hatnean, J. A.; Johnson, S. A. Synthesis and chemistry of bis(triisopropylphosphine) nickel(I) and nickel(0) precursors. *Dalton Trans.* **2013**, *42*, 1461-1475; (c) Zhu, S.; Shoshani, M. M.; Johnson, S. A. Versatile $(\eta^6\text{-arene})Ni(PCy_3)$ nickel monophosphine precursors. *Chem. Commun.* **2017**, *53*, 13176-13179.

(8) For reviews, see: (a) Colacot, T. J. A Highly Active Palladium(I) Dimer for Pharmaceutical Applications. *Platinum Met. Rev.* **2009**, *53*, 183-188; (b) Fricke, C.; Sperger, T.; Mendel, M.; Schoenebeck, F. Catalysis with Palladium(I) Dimers. *Angew. Chem. Int. Ed.* **2021**, *60*, 3355-3366.

(9) (a) Stambuli, J. P.; Kuwano, R.; Hartwig, J. F. Unparalleled Rates for the Activation of Aryl Chlorides and Bromides: Coupling with Amines and Boronic Acids in Minutes at Room Temperature. *Angew. Chem. Int. Ed.* **2002**, *41*, 4746-4748; (b) Hama, T.; Liu, X.; Culkin, D. A.; Hartwig, J. F. Palladium-Catalyzed α-Arylation of Esters and Amides under More Neutral Conditions. *J. Am. Chem. Soc.* **2003**, *125*, 11176-11177; (c) Prashad, M.; Mak, X. Y.; Liu, Y.; Repič, O. Palladium-Catalyzed Amination of Aryl Bromides with Hindered N-Alkyl-Substituted Anilines Using a Palladium(I) Tri-*tert*-butylphosphine Bromide Dimer. *J. Org. Chem.* **2003**, *68*, 1163-1164; (d) Hill, L. L.; Crowell, J. L.; Tutwiler, S. L.; Massie, N. L.; Hines, C. C.; Griffin, S. T.; Rogers, R. D.; Shaughnessy, K. H.; Grasa, G. A.; Johansson Seechurn, C.C.C.; Li, H.; Colacot, T.; Chou, J.; Woltermann, C. J. Synthesis and X-ray Structure Determination of Highly Active Pd(II), Pd(I), and Pd(0) Complexes of Di(*tert*-butyl)neopentylphosphine (DTBNpP) in the Arylation of Amines and Ketones. *J. Org. Chem.* **2010**, *75*, 6477-6488; (e) Proutiere, F.; Aufiero, M.; Schoenebeck, F. Reactivity and Stability of Dinuclear Pd(I) Complexes: Studies on the Active Catalytic Species, Insights into Precatalyst Activation and Deactivation, and Application in Highly Selective Cross-Coupling Reactions. *J. Am. Chem. Soc.* **2012**, *134*, 606-612.

(10) (a) Aufiero, M.; Proutiere, F.; Schoenebeck, F. Redox Reactions in Palladium Catalysis: On the Accelerating and/or Inhibiting Effects of Copper and Silver Salt Additives in Cross-Coupling Chemistry Involving Electron-rich Phosphine Ligands. *Angew. Chem. Int. Ed.* **2012**, *51*, 7226-7230; (b) Guard, L. M.; Mohadjer Beromi, M.; Brudvig, G. W.; Hazari, N.; Vinyard, D. J. Comparison of dppf-Supported Nickel Precatalysts for the Suzuki–Miyaura Reaction: The Observation and Activity of Nickel(I). *Angew. Chem. Int. Ed.* **2015**, *54*, 13352-13356; (c) Melvin, P. R.; Nova, A.; Balcells, D.; Dai, W.; Hazari, N.; Hruszkewycz, D. P.; Shah, H. P.; Tudge, M. T. Design of a Versatile and Improved Precatalyst Scaffold for Palladium-Catalyzed Cross-Coupling: $(\eta^3\text{-}1\text{-}^t\text{Bu-indenyl})_2(\mu\text{-Cl})_2Pd_2$. *ACS Catal.* **2015**, *5*, 3680-3688; (d) Johansson Seechurn, C. C. C.; Sperger, T.; Scrase, T. G.; Schoenebeck, F.; Colacot, T. J. Understanding the Unusual Reduction Mechanism of Pd(II) to Pd(I): Uncovering Hidden Species and Implications in Catalytic Cross-Coupling Reactions. *J. Am. Chem. Soc.* **2017**, *139*, 5194-5200.

(11) Aufiero, M.; Scattolin, T.; Proutière, F.; Schoenebeck, F. Air-Stable Dinuclear Iodine-Bridged Pd(I) Complex - Catalyst, Precursor, or Parasite? The Additive Decides. Systematic Nucleophile-Activity Study and Application as Precatalyst in Cross-Coupling. *Organometallics* **2015**, *34*, 5191-5195.

(12) For examples of direct reactivity of $Pd^{(I)}$-$Pd^{(I)}$, see: (a) Bonney, K. J.; Proutiere, F.; Schoenebeck, F. Dinuclear Pd(I) complexes—solely precatalysts? Demonstration of direct reactivity of a Pd(I) dimer with an aryl iodide. *Chem. Sci.* **2013**, *4*, 4434-4439; (b) Kalvet, I.; Bonney, K. J.; Schoenebeck, F. Kinetic and Computational Studies on Pd(I) Dimer-Mediated Halogen Exchange of Aryl Iodides. *J. Org. Chem.* **2014**, *79*, 12041-12046; (c) Aufiero, M.; Sperger, T.; Tsang, A. S.-K.; Schoenebeck, F. Highly Efficient C-$SeCF_3$ Coupling of Aryl Iodides Enabled by an Air-Stable Dinuclear Pd^I Catalyst. *Angew. Chem. Int. Ed.* **2015**, *54*, 10322-10326; (d) Yin, G.; Kalvet, I.; Schoenebeck, F. Trifluoromethylthiolation of Aryl Iodides and Bromides Enabled by a Bench-Stable and Easy-To-Recover Dinuclear Palladium(I) Catalyst. *Angew. Chem. Int. Ed.* **2015**, *54*, 6809-6813; (e)

Scattolin, T.; Senol, E.; Yin, G.; Guo, Q.; Schoenebeck, F. Site-Selective C−S Bond Formation at C−Br over C−OTf and C−Cl Enabled by an Air-Stable, Easily Recoverable, and Recyclable Palladium(I) Catalyst. *Angew. Chem. Int. Ed.* **2018**, *57*, 12425-12429; (f) Chen, X.-Y.; Pu, M.; Cheng, H.-G.; Sperger, T.; Schoenebeck, F. Arylation of Axially Chiral Phosphorothioate Salts by Dinuclear Pd^{I} Catalysis. *Angew. Chem. Int. Ed.* **2019**, *58*, 11395-11399.

(13) For selected reviews, see: (a) Powers, I. G.; Uyeda, C. Metal–Metal Bonds in Catalysis. *ACS Catal.* **2017**, *7*, 936-958; (b) Lin, C.-Y.; Power, P. P. Complexes of Ni(I): a "rare" oxidation state of growing importance. *Chem. Soc. Rev.* **2017**, *46*, 5347-5399; (c) Bismuto, A.; Finkelstein, P.; Müller, P.; Morandi, B. The Journey of Ni(I) Chemistry. *Helv. Chim. Acta* **2021**, *104*, e2100177.

(14) For selected examples of trialkylphosphine-based $Ni^{(I)}$ dimers with other bridges than dihalogen, see: (a) Deppisch, B.; Schäfer, H. Übergangsmetallphosphidokomplexe. VI. Die Struktur von Bis(μ-bistrimethylsilylphosphido)-bis(trimethylphosphinnickel) $[Me_3PNiP(SiMe_3)_2]_2$, einem phosphidoverbrückten Phosphinkomplex mit trigonal planar koordiniertem Nickel(I). *Z. anorg. allg. Chem.* **1982**, *490*, 129-135; (b) Jones, R. A.; Stuart, A. L.; Atwood, J. L.; Hunter, W. E.; Rogers, R. D. Steric effects of phosphido ligands. Synthesis and crystal structures of bis(tert-butylphosphido)-bridged dinuclear metal-metal-bonded complexes of iron(II), cobalt(I, II) and nickel(I). *Organometallics* **1982**, *1*, 1721-1723; (c) Kriley, C. E.; Woolley, C. J.; Krepps, M. K.; Popa, E. M.; Fanwick, P. E.; Rothwell, I. P. Synthesis and characterization of a series of novel nickel(II)/nickel(I) complexes. Crystal structures of $[NiCl_2(dcpm)]$, $[Ni(dcpm)_2](NO_3)_2{\cdot}2EtOH$, $[Ni_2Cl_2(\mu\text{-}dcpm)_2(\mu\text{-}H)]$ and $[Ni_2(\mu\text{-}PCy_2)_2(PCy_2Me)_2]$; dcpm=bis(dicyclohexylphosphino)methane. *Inorganica Chim. Acta* **2000**, *300-302*, 200-205; (d) Haehnel, M.; Hansen, S.; Schubert, K.; Arndt, P.; Spannenberg, A.; Jiao, H.; Rosenthal, U. Synthesis, Characterization and Reactivity of Group 4 Metallocene Bis(diphenylphosphino)acetylene Complexes—A Reactivity and Bonding Study. *J. Am. Chem. Soc.* **2013**, *135*, 17556-17565; (e) Chen, Y.; Sui-Seng, C.; Zargarian, D. Tetraphenylborate as a Novel Bridging Ligand in a Zwitterionic Nickel(I) Dimer. *Angew. Chem. Int. Ed.* **2005**, *44*, 7721-7725; For selected examples of other types of phosphine-derived $Ni^{(I)}$ dimers with other bridges than dihalogen, see: (f) Ito, M.; Matsumoto, T.; Tatsumi, K. Synthesis and Reactions of Mono- and Dinuclear Ni(I) Thiolate Complexes. *Inorg. Chem.* **2009**, *48*, 2215-2223; (g) Beck, R.; Johnson, S. A. Dinuclear Ni(I)-Ni(I) Complexes with Syn-Facial Bridging Ligands from Ni(I) Precursors or Ni(II)/Ni(0) Comproportionation. *Organometallics* **2013**, *32*, 2944-2951; For trialkylphosphine-derived $Ni^{(I)}$ dimers with one halogen-bridge, see: (h) Bismuto, A.; Müller, P.; Finkelstein, P.; Trapp, N.; Jeschke, G.; Morandi, B. One to Find Them All: A General Route to Ni(I)–Phenolate Species. *J. Am. Chem. Soc.* **2021**, *143*, 10642-10648.

(15) For an example of a dihalogen-bridged $Ni^{(I)}$ dimer that carries phosphine ligands other than bulky trialkyl, see: Newman-Stonebraker, S. H.; Wang, J. Y.; Jeffrey, P. D.; Doyle, A. G. Structure–Reactivity Relationships of Buchwald-Type Phosphines in Nickel-Catalyzed Cross-Couplings. *J. Am. Chem. Soc.* **2022**, *144*, 19635-19648.

(16) Dible, B. R.; Sigman, M. S.; Arif, A. M. Oxygen-Induced Ligand Dehydrogenation of a Planar Bis-μ-Chloronickel(I) Dimer Featuring an NHC Ligand. *Inorg. Chem.* **2005**, *44*, 3774-3776.

(17) (a) Dürr, A. B.; Fisher, H. C.; Kalvet, I.; Truong, K.-N.; Schoenebeck, F. Divergent Reactivity of a Dinuclear (NHC)Nickel(I) Catalyst versus Nickel(0) Enables Chemoselective Trifluoromethylselenolation. *Angew. Chem. Int. Ed.* **2017**, *56*, 13431-13435; (b) Matsubara, K.; Yamamoto, H.; Miyazaki, S.; Inatomi, T.; Nonaka, K.; Koga, Y.; Yamada, Y.; Veiros, L. F.; Kirchner, K. Dinuclear Systems in the Efficient Nickel-Catalyzed Kumada–Tamao–Corriu Cross-Coupling of Aryl Halides. *Organometallics* **2017**, *36*, 255-265; (c) Kapat, A.; Sperger, T.; Guven, S.; Schoenebeck, F. E-Olefins through intramolecular radical relocation. *Science* **2019**, *363*, 391-396; (d) Liu, C.-F.; Wang, H.; Martin, R. T.; Zhao, H.; Gutierrez, O.; Koh, M. J. Olefin functionalization/isomerization enables stereoselective alkene synthesis. *Nature Catal.* **2021**, *4*, 674-683; (e) Wang, H.; Liu, C.-F.; Martin, R. T.; Gutierrez, O.; Koh, M. J. Directing-group-free catalytic dicarbofunctionalization of unactivated alkenes. *Nat. Chem.* **2022**, *14*, 188-195.

(18) For recent examples of applications of machine learning (or data science) in organometallic catalysis and speciation, see: (a) Gao, H.; Struble, T. J.; Coley, C. W.; Wang, Y.; Green, W. H.; Jensen, K. F. Using Machine Learning To Predict Suitable Conditions for Organic Reactions. *ACS Cent. Sci.* **2018**, *4*, 1465-1476; (b) Cordova, M.; Wodrich, M. D.; Meyer, B.; Sawatlon, B.; Corminboeuf, C. Data-Driven Advancement of Homogeneous Nickel Catalyst Activity for Aryl Ether Cleavage. *ACS Catal.* **2020**, *10*, 7021-7031; (c) Friederich, P.; dos Passos Gomes, G.; De Bin, R.; Aspuru-Guzik, A.; Balcells, D. Machine learning dihydrogen activation in the chemical space surrounding Vaska's complex. *Chem. Sci.* **2020**, *11*, 4584-4601; (d) Gadekar, S. C.; Dhayalan, V.; Nandi, A.; Zak, I. L.; Mizrachi, M. S.; Kozuch, S.; Milo, A. Rerouting the Organocatalytic Benzoin Reaction toward Aldehyde Deuteration. *ACS Catal.* **2021**, *11*, 14561-14569; (e) Żurański, A. M.; Martinez Alvarado, J. I.; Shields, B. J.; Doyle, A. G. Predicting Reaction Yields via Supervised Learning. *Acc. Chem. Res.* **2021**, *54*, 1856-1865; (f) DeLano, T. J.; Dibrell, S. E.; Lacker, C. R.; Pancoast, A. R.; Poremba, K. E.; Cleary, L.; Sigman, M. S.; Reisman, S. E. Nickel-catalyzed asymmetric reductive cross-coupling of α-chloroesters with (hetero)aryl iodides. *Chem. Sci.* **2021**, *12*, 7758-7762; When we embarked on our research, the LKB-P was the most comprehensive database for monodentate phosphines. However, in the mean time a more extensive database has been published, called kraken: (g) Gensch, T.; dos Passos Gomes, G.; Friederich, P.; Peters, E.; Gaudin, T.; Pollice, R.; Jorner, K.; Nigam, A.; Lindner-D'Addario, M.; Sigman, M. S.; Aspuru-Guzik, A. A Comprehensive Discovery Platform for Organophosphorus Ligands for Catalysis. *J. Am. Chem. Soc.* **2022**, *144*, 1205-1217.

(19) For recent applications of unsupervised machine learning in organometallic catalysis, see: (a) Kariofillis, S. K.; Jiang, S.; Żurański, A. M.; Gandhi, S. S.; Martinez Alvarado, J. I.; Doyle, A. G. Using Data Science To Guide Aryl Bromide Substrate Scope Analysis in a Ni/Photoredox-Catalyzed Cross-Coupling with Acetals as Alcohol-Derived Radical Sources. *J. Am. Chem. Soc.* **2022**, *144*, 1045-1055; (b) Lacker, C. R.; DeLano, T. J.; Chen, E. P.; Kong, J.; Belyk, K. M.; Piou, T.; Reisman, S. E. Enantioselective Synthesis of N-Benzylic Heterocycles by Ni/Photoredox Dual Catalysis. *J. Am. Chem. Soc.* **2022**, *144*, 20190-20195; (c) Gensch, T.; Smith, S. R.; Colacot, T. J.; Timsina, Y. N.; Xu, G.; Glasspoole, B. W.; Sigman, M. S. Design and Application of a Screening Set for Monophosphine Ligands in Cross-Coupling. *ACS Catal.* **2022**, *12*, 7773-7780; (d) Rose, B. T.; Timmerman, J. C.; Bawel, S. A.; Chin, S.; Zhang, H.; Denmark, S. E. High-Level Data Fusion Enables the Chemoinformatically Guided Discovery of Chiral Disulfonimide Catalysts for Atropselective Iodination of 2-Amino-6-arylpyridines. *J. Am. Chem. Soc.* **2022**, *144*, 22950-22964.

(20) For recent reviews on the application of machine-learning in catalysis, see: (a) Toyao, T.; Maeno, Z.; Takakusagi, S.; Kamachi, T.; Takigawa, I.; Shimizu, K.-i. Machine Learning for Catalysis Informatics: Recent Applications and Prospects. *ACS Catal.* **2020**, *10*, 2260-2297; (b) Zahrt, A. F.; Athavale, S. V.; Denmark, S. E. Quantitative Structure–Selectivity Relationships in Enantioselective Catalysis: Past, Present, and Future. *Chem. Rev.* **2020**, *120*, 1620-1689; (c) Funes-Ardoiz, I.; Schoenebeck, F. Established and Emerging Computational Tools to Study Homogeneous Catalysis—From Quantum Mechanics to Machine Learning. *Chem* **2020**, *6*, 1904-1913; (d) dos Passos Gomes, G.; Pollice, R.; Aspuru-Guzik, A. Navigating through the Maze of Homogeneous Catalyst Design with Machine Learning. *Trends in Chemistry* **2021**, *3*, 96-110; (e) Jorner, K.; Tomberg, A.; Bauer, C.; Sköld, C.; Norrby, P.-O. Organic reactivity from mechanism to machine learning. *Nat. Rev. Chem.* **2021**, *5*, 240-255; (f) Williams, W. L.; Zeng, L.; Gensch, T.; Sigman, M. S.; Doyle, A. G.; Anslyn, E. V. The Evolution of Data-Driven Modeling in Organic Chemistry. *ACS Cent. Sci.* **2021**, *7*, 1622-1637; (g) Lustosa, D. M.; Milo, A. Mechanistic Inference from Statistical Models at Different Data-Size Regimes. *ACS Catal.* **2022**, *12*, 7886-7906; (h) Mai, H.; Le, T. C.; Chen, D.; Winkler, D. A.; Caruso, R. A. Machine Learning for Electrocatalyst and Photocatalyst Design and Discovery. *Chem. Rev.* **2022**, *122*, 13478-13515; (i) Tu, Z.; Stuyver, T.; Coley, C.

W. Predictive chemistry: machine learning for reaction deployment, reaction development, and reaction discovery. *Chem. Sci.* **2023**, *14*, 226-244.

(21) It has been achieved with Pd-trimers, see: Diehl, C. J.; Scattolin, T.; Englert, U.; Schoenebeck, F. C-I-Selective Cross-Coupling Enabled by a Cationic Palladium Trimer. *Angew. Chem. Int. Ed.* **2019**, *58*, 211-215.

(22) Hueffel, J. A.; Sperger, T.; Funes-Ardoiz, I.; Ward, J. S.; Rissanen, K.; Schoenebeck, F. Accelerated dinuclear palladium catalyst identification through unsupervised machine learning. *Science* **2021**, *374*, 1134-1140.

(23) (a) Jover, J.; Fey, N.; Harvey, J. N.; Lloyd-Jones, G. C.; Orpen, A. G.; Owen-Smith, G. J. J.; Murray, P.; Hose, D. R. J.; Osborne, R.; Purdie, M. Expansion of the Ligand Knowledge Base for Monodentate P-Donor Ligands (LKB-P). *Organometallics* **2010**, *29*, 6245-6258; (b) Fey, N.; Tsipis, A. C.; Harris, S. E.; Harvey, J. N.; Orpen, A. G.; Mansson, R. A. Development of a Ligand Knowledge Base, Part 1: Computational Descriptors for Phosphorus Donor Ligands. *Chem. Eur. J.* **2006**, *12*, 291-302.

(24) Some methods for classification and analysis of multivariate observations

(25) Hua, J.; Xiong, Z.; Lowey, J.; Suh, E.; Dougherty, E. R. Optimal number of features as a function of sample size for various classification rules. *Bioinformatics* **2005**, *21*, 1509-1515.

(26) For **L3**, **L8** and **L16** there are a few reports of uses in Pd-catalysis, see: (a) Mann, G.; Incarvito, C.; Rheingold, A. L.; Hartwig, J. F. Palladium-Catalyzed C−O Coupling Involving Unactivated Aryl Halides. Sterically Induced Reductive Elimination To Form the C−O Bond in Diaryl Ethers. *J. Am. Chem. Soc.* **1999**, *121*, 3224-3225; (b) Wolkowski, J. P.; Hartwig, J. F. Generation of Reactivity from Typically Stable Ligands: C-C Bond-Forming Reductive Elimination from Aryl Palladium(II) Complexes of Malonate Anions. *Angew. Chem. Int. Ed.* **2002**, *41*, 4289-4291; (c) Qu, B.; Haddad, N.; Han, Z. S.; Rodriguez, S.; Lorenz, J. C.; Grinberg, N.; Lee, H.; Busacca, C. A.; Krishnamurthy, D.; Senanayake, C. H. Palladium-catalyzed aminocarbonylation of heteroaryl halides using di-*tert*-butylphosphinoferrocene. *Tetrahedron Lett.* **2009**, *50*, 6126-6129; (d) Milde, B.; Lohan, M.; Schreiner, C.; Rüffer, T.; Lang, H. (Metallocenylphosphane)palladium Dichlorides – Synthesis, Electrochemistry and Their Application in C–C Coupling Reactions. *Eur. J. Inorg. Chem.* **2011**, *2011*, 5437-5449; (e) Ullah, E.; McNulty, J.; Sliwinski, M.; Robertson, A. One-step synthesis of reusable, polymer-supported tri-alkyl phosphine ligands. Application in Suzuki–Miyaura and alkoxycarbonylation reactions. *Tetrahedron Lett.* **2012**, *53*, 3990-3993; (f) Ge, S.; Arlow, S. I.; Mormino, M. G.; Hartwig, J. F. Pd-Catalyzed α-Arylation of Trimethylsilyl Enolates of α,α-Difluoroacetamides. *J. Am. Chem. Soc.* **2014**, *136*, 14401-14404.

(27) (a) Fleckenstein, C. A.; Plenio, H. 9-Fluorenylphosphines for the Pd-Catalyzed Sonogashira, Suzuki, and Buchwald–Hartwig Coupling Reactions in Organic Solvents and Water. *Chem. Eur. J.* **2007**, *13*, 2701-2716; (b) Fleckenstein, C. A.; Plenio, H. The Role of Bidentate Fluorenylphosphines in Palladium-Catalyzed Cross-Coupling Reactions. *Organometallics* **2008**, *27*, 3924-3932.

(28) Payard, P.-A.; Perego, L. A.; Grimaud, L.; Ciofini, I. A DFT Protocol for the Prediction of 31P NMR Chemical Shifts of Phosphine Ligands in First-Row Transition-Metal Complexes. *Organometallics* **2020**, *39*, 3121-3130.

(29) For reactions in benzene, $NiBr_2$(dme) and phosphine were mixed and stirred for 45 min to 4 h. Then a solution of $Ni(cod)_2$ in benzene was added and the reactions monitored by ^{31}P NMR. Due to greater solubility in THF, only 1 min mixing of reagents was sufficient.

(30) THF again had a pronounced impact on the ^{31}P shifts. The measured ^{31}P signals of the THF reaction mixtures were δ = 104.2 ppm for **D2**, δ = 113.9 ppm for **D3**, δ = 100.1 ppm for **D8**, δ = 113.0 ppm for **D9** and δ = 76.8 ppm for **D17**. Note that for **D9** and **D17** in both benzene and THF free ligand was observed alongside the newly formed species.

(31) Deposition numbers 2265372 (for **D2**), 2252179 (for **D3**), 2265373 (for **D4**), 2252180 (for **D5**), 2265374 (for **D6**), 2265375 (for **D7**), 2252146 (for **D8**), 2265472 (for **D9**), 2252211 (for **D12**), 2252181 (for **D13**), 2252147 (for **D16**) and 2265376 (for **D17**) contain the supplementary crystallographic data for this paper. These data are provided free of charge by the joint Cambridge Crystallographic Data Centre and Fachinformationszentrum Karlsruhe Access Structures service.

(32) Also for these, THF had a pronounced impact on the ^{31}P shifts. The measured ^{31}P signals of the THF reaction mixtures were δ = 88.6 ppm for **D4**, δ = 110.7 ppm for **D6**, δ = 125.8 ppm for **D13** and δ = 79.6 ppm for **D16**.

(33) Given the similarity of **L15** to **L16**, and the fact that **L15** requires a 5-step synthesis and is not our primary target (i.e. trialkylphosphine-derived Ni(I) dimers), we did not experimentally test **L15**.

(34) Alongside the observed dominant species, free ligand was detected in the NMR.

(35) For reviews, see: (a) Almond-Thynne, J.; Blakemore, D. C.; Pryde, D. C.; Spivey, A. C. Site-selective Suzuki–Miyaura coupling of heteroaryl halides – understanding the trends for pharmaceutically important classes. *Chem. Sci.* **2017**, *8*, 40-62; (b) Palani, V.; Perea, M. A.; Sarpong, R. Site-Selective Cross-Coupling of Polyhalogenated Arenes and Heteroarenes with Identical Halogen Groups. *Chem. Rev.* **2022**, *122*, 10126-10169.

(36) (a) Kalvet, I.; Sperger, T.; Scattolin, T.; Magnin, G.; Schoenebeck, F. Palladium(I) Dimer Enabled Extremely Rapid and Chemoselective Alkylation of Aryl Bromides over Triflates and Chlorides in Air. *Angew. Chem. Int. Ed.* **2017**, *56*, 7078-7082; (b) Kalvet, I.; Magnin, G.; Schoenebeck, F. Rapid Room-Temperature, Chemoselective C −C Coupling of Poly(pseudo)halogenated Arenes Enabled by Palladium(I) Catalysis in Air. *Angew. Chem. Int. Ed.* **2017**, *56*, 1581-1585; (c) Keaveney, S. T.; Kundu, G.; Schoenebeck, F. Modular Functionalization of Arenes in a Triply Selective Sequence: Rapid C(sp2) and C(sp3) Coupling of C−Br, C−OTf, and C−Cl Bonds Enabled by a Single Palladium(I) Dimer. *Angew. Chem. Int. Ed.* **2018**, *57*, 12573-12577; (d) Sperger, T.; Schoenebeck, F. α-Arylation of Esters and Ketones Enabled by a Bench-Stable Pd(I) Dimer Catalyst. *Synth.* **2018**, *50*, 4471-4475; (e) Kalvet, I.; Deckers, K.; Funes-Ardoiz, I.; Magnin, G.; Sperger, T.; Kremer, M.; Schoenebeck, F. Selective ortho-Functionalization of Adamantylarenes Enabled by Dispersion and an Air-Stable Palladium(I) Dimer. *Angew. Chem. Int. Ed.* **2020**, *59*, 7721-7725; (f) Kundu, G.; Sperger, T.; Rissanen, K.; Schoenebeck, F. A Next-Generation Air-Stable Palladium(I) Dimer Enables Olefin Migration and Selective C−C Coupling in Air. *Angew. Chem. Int. Ed.* **2020**, *59*, 21930-21934; (g) Mendel, M.; Kalvet, I.; Hupperich, D.; Magnin, G.; Schoenebeck, F. Site-Selective, Modular Diversification of Polyhalogenated Aryl Fluorosulfates ($ArOSO_2F$) Enabled by an Air-Stable Pd^I Dimer. *Angew. Chem. Int. Ed.* **2020**, *59*, 2115-2119; (h) Kreisel, T.; Mendel, M.; Queen, A. E.; Deckers, K.; Hupperich, D.; Riegger, J.; Fricke, C.; Schoenebeck, F. Modular Generation of (Iodinated) Polyarenes Using Triethylgermane as Orthogonal Masking Group. *Angew. Chem. Int. Ed.* **2022**, *61*, e202201475.

(37) Lin, K.; Wiles, R. J.; Kelly, C. B.; Davies, G. H. M.; Molander, G. A. Haloselective Cross-Coupling via Ni/Photoredox Dual Catalysis. *ACS Catal.* **2017**, *7*, 5129-5133.

(38) For selected examples, see: (a) Li, X.; Feng, Z.; Jiang, Z.-X.; Zhang, X. Nickel-Catalyzed Reductive Cross-Coupling of (Hetero)Aryl Iodides with Fluorinated Secondary Alkyl Bromides. *Org. Lett.* **2015**, *17*, 5570-5573; (b) Sheng, J.; Ni, H.-Q.; Zhang, H.-R.; Zhang, K.-F.; Wang, Y.-N.; Wang, X.-S. Nickel-Catalyzed Reductive Cross-Coupling of Aryl Halides with Monofluoroalkyl Halides for Late-Stage Monofluoroalkylation. *Angew. Chem. Int. Ed.* **2018**, *57*, 7634-7639; (c) Shu, W.; García-Domínguez, A.; Quirós, M. T.; Mondal, R.; Cárdenas, D. J.; Nevado, C. Ni-Catalyzed Reductive Dicarbofunctionalization of Nonactivated Alkenes: Scope and Mechanistic Insights. *J. Am. Chem. Soc.* **2019**, *141*, 13812-13821; (d) Charboneau, D. J.; Barth, E. L.; Hazari, N.; Uehling, M. R.; Zultanski, S. L. A Widely Applicable Dual Catalytic System for Cross-Electrophile Coupling Enabled by Mechanistic Studies. *ACS Catal.* **2020**, *10*, 12642-12656; (e) Watanabe, E.; Chen, Y.; May, O.; Ley, S. V. A Practical Method for Continuous Production of sp3-Rich Compounds from (Hetero)Aryl Halides and Redox-Active Esters. *Chem. Eur. J.* **2020**, *26*, 186-191; (f) Gabbey, A. L.; Michel, N. W. M.; Hughes, J. M. E.; Campeau, L.-C.; Rousseaux, S. A. L. Synthesis of α-

Aryl Secondary Amides via Nickel-Catalyzed Reductive Coupling of Redox-Active Esters. *Org. Lett.* **2022**, *24*, 3173-3178; (g) Li, Y.; Wang, Z.; Li, L.; Tian, X.; Shao, F.; Li, C. Chemoselective and Diastereoselective Synthesis of C-Aryl Nucleoside Analogues by Nickel-Catalyzed Cross-Coupling of Furanosyl Acetates with Aryl Iodides. *Angew. Chem. Int. Ed.* **2022**, *61*, e202110391; (h) Zhu, C.; Lee, S.-C.; Chen, H.; Yue, H.; Rueping, M. Reductive Cross-Coupling of α-Oxy Halides Enabled by Thermal Catalysis, Photocatalysis, Electrocatalysis, or Mechanochemistry. *Angew. Chem. Int. Ed.* **2022**, *61*, e202204212; For selected examples of selective C-S and C-N bond formations, see: (i) Liu, Y.; Xing, S.; Zhang, J.; Liu, W.; Xu, Y.; Zhang, Y.; Yang, K.; Yang, L.; Jiang, K.; Shao, X. Construction of diverse C–S/C–Se bonds via nickel catalyzed reductive coupling employing thiosulfonates and a selenosulfonate under mild conditions. *Org. Chem. Front.* **2022**, *9*, 1375-1382; (j) Peng, K.; Gao, M.-Y.; Yi, Y.-Y.; Guo, J.; Dong, Z.-B. Copper/Nickel-Catalyzed Selective C–S/S–S Bond Formation Starting from O-Alkyl Phenylcarbamothioates. *Eur. J. Org. Chem.* **2020**, *2020*, 1665-1672; (k) Dhital, R. N.*;* Sen, A.; Hu, H.; Ishii, R.; Sato, T.; Yashiroda, Y.; Kimura, H.; Boone, C.; Yoshida, M.; Futamura, Y.; Hirano, H.; Osada, H.; Hashizume, D.; Uozumi, Y.; Yamada, Y. M. A. Phenylboronic Ester-Activated Aryl Iodide-Selective Buchwald–Hartwig-Type Amination toward Bioactivity Assay. *ACS Omega* **2022**, *7*, 24184-24189.

(39) Prior to purification the crude reactions were analysed by GC-MS. In some cases, small amounts of starting material (up to 6%) and bisfunctionalization (<4%) were detected. For substrate **5**, 9% of SM and 1% of bisfunctionalization were detected. For further details see SI.

(40) The duration of those ^{31}P NMR measurements was 4 min.

(41) While subjection of 1 equiv. of substrate to this new species only leads to 10% conversion to product, addition of an additional equivalent of Grignard reagent along with substrate gives the coupling product in high yield.

(42) Borys, A. M.; Hevia, E. The Anionic Pathway in the Nickel-Catalysed Cross-Coupling of Aryl Ethers. *Angew. Chem. Int. Ed.* **2021**, *60*, 24659-24667.

(43) For the reaction of $Ni(COD)_2$/PAd_2(*n*-Bu), after 1.5 h reaction time, there is still 53% of starting material and 29% of deiodinated starting material as well as 12% of coupling product. For the same reaction with [(TMEDA)Ni(o-tol)Cl]/PAd_2(*n*-Bu) after 2h, there is 52% of starting material, 44% of deiodinated byproduct and only 2% of coupling product.

Table of Contents (TOC)